Sensors and Actuators A 263 (2017) 493–500

Contents lists available at ScienceDirect

Sensors and Actuators A: Physical

journal homepage: www.elsevier.com/locate/sna

# 3D printing of multiaxial force sensors using carbon nanotube (CNT)/thermoplastic polyurethane (TPU) filaments

Kyuyoung Kim, Jaeho Park, Ji-hoon Suh, Minseong Kim, Yongrok Jeong, Inkyu Park*

*Department of Mechanical Engineering, Korea Advanced Institute of Science and Technology, 291 Daehak-ro, Yuseong-gu, Daejeon 34141, Republic of Korea*

ARTICLE INFO

*Article history:*
Received 6 April 2017
Received in revised form 7 July 2017
Accepted 10 July 2017
Available online 13 July 2017

*Keywords:*
3D printing
3D-printed sensor
Fused deposition modeling
Multiaxial force sensor
Piezoresistivity
Nanocomposite filament

ABSTRACT

We developed a new method to directly fabricate 3D multiaxial force sensor using fused deposition modeling (FDM) 3D printing of functionalized nanocomposite filaments. Here, 3D cubic cross shaped force sensor is suggested to measure the forces from three axes (x, y and z). The sensor has two components – a structural part and a sensing part – both of which are concurrently fabricated by 3D printing with different functional filaments. The structural part is printed with thermoplastic polyurethane (TPU) filament and the sensing part is printed with carbon nanotube (CNT)/TPU nanocomposite filament with a piezoresistivity on the surface of the structural part. The resistances of the sensing part are measured in three axial directions; $R_x$, $R_y$, and $R_z$ and the force applied on each axis is measured by the resistance change. The 3D-printed multiaxial force sensor could detect the sub-millimeter scale deflection and its corresponding force on each axis. According to the sensing principle, when $F_z = 4$ N was applied, $R_z$ was decreased by 2% while only 0.2% resistance change of $R_y$ was induced. In addition, a simultaneous resistance measurement system was developed for a real-time force sensing in three axes. With its customizability, rapid manufacturing, and economic feasibility, this manufacturing approach allows direct fabrication of multiaxial sensors without additional assembly or integration processes.



## 1. Introduction

Three-dimensional printing (3DP), also known as additive manufacturing (AM) is a technology that enables the printing of three dimensional objects layer by layer. Fused deposition modeling (FDM) is the most widespread 3DP technology due to its simple working principle and cost-effective manufacturing process as compared to other methods such as stereolithography (SLA) and selective laser sintering (SLS). Also, many materials could be 3D printed with FDM. FDM usually utilizes thermoplastic materials such as acrylonitrile butadiene styrene (ABS) or polylactic acid (PLA), however, various 3D printable composites have also been developed [1,2]. Many researchers nowadays try to broaden the field of FDM 3DP applications by fabricating functional objects with various composite materials and 3D printing's design versatility.

Recent works on the fabrication of functional objects with FDM 3D printing exist in two different approaches. One approach is to fabricate structural parts first with 3D printing and then to embed functional devices such as electrical or fluidic components that were pre-fabricated by conventional manufacturing methods [3–10]. This approach uses 3D-printed structure only as a structural frame where functional devices can be attached or inserted. Another approach is to print functional objects directly using composite materials [11–16]. Because FDM 3DP can use various thermoplastic composite materials, many different types of functional objects can be directly fabricated by this method. For example, a hygroscopic actuator was printed with a cellulose filament [11,12] and a capacitive touch sensor was printed with a conductive filament for human-computer interaction [13]. Also, liquid sensors with 3D-printed nanocomposite were developed for detecting dichloromethane (DCM), methanol, etc. [17,18].

This approach has been applied to 3D printing of force sensors. G. Peterson, et al. [19], showed that a 3D-printed mechanochromic material could be used for the force sensor. The tensile force applied to the sensor could be evaluated by the color change, but the process was irreversible and only qualitative analysis was possible. On the other hand, S. Leigh, et al. [20], developed carbon black/polycaprolactone (PCL) filaments and printed them on the 3D-printed glove as line patterns for the detection of finger motion by measuring the resistance change. However, it could be fabricated by conventional 2D printing methods without utilizing 3D printing because it was only two dimensional. Also, it was not suitable for a large motion sensing since the printed material was not sufficiently flexible.

* Corresponding author.
*E-mail address:* inkyu@kaist.ac.kr (I. Park).

http://dx.doi.org/10.1016/j.sna.2017.07.020
0924-4247/

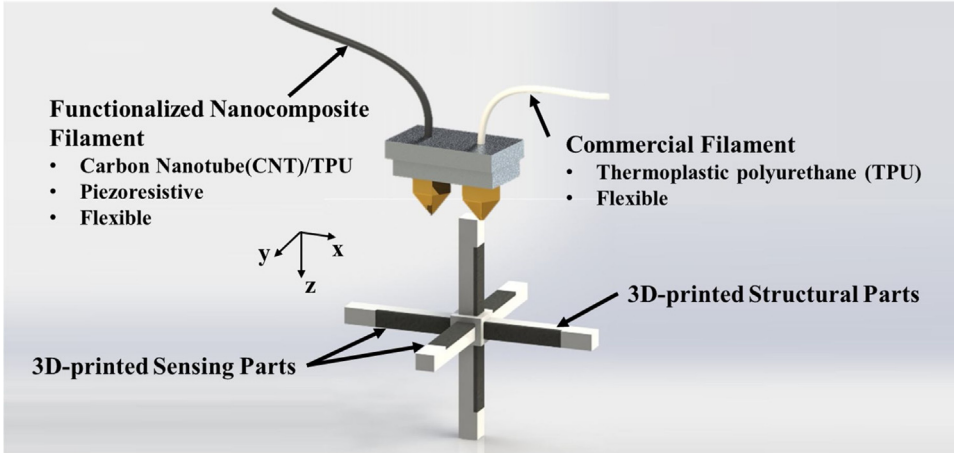


**Fig. 1.** Schematic design of 3D-printed multiaxial force sensor and its fabrication principle based on the simultaneous fused deposition modeling (FDM) type 3D printing of sensing and structural materials.

Here, we report a 3D-printed multiaxial force sensor that can measure the forces in three orthogonal axes. It has a unique 3D cubic cross structure with two different components – sensing and structural parts. The sensing part senses the mechanical inputs to the sensor by its resistance change while the structural part provides the physical platform for the sensors. For the sensing part, we fabricated a functionalized nanocomposite filament composed of carbon nanotube (CNT) and thermoplastic polyurethane (TPU) that has mechanical flexibility, electrical conductivity and piezoresistivity. The sensor is printed by a commercial FDM 3D printer which could alternately print TPU filament for the structural part and CNT/TPU composite filament for the sensing part. Although FDM 3D printing is known for its low printing quality, it is used for its various advantages: ease of use, low fabrication cost, and compatibility with various composite materials. Since CNT/TPU was printed as a sensing material, FDM was chosen as the most suitable and straightforward method to be used to achieve the goal. The sensor realizes multiaxial force sensing owing to its 3D cubic cross structure, in which each beam measures the force applied in three individual axes (see Fig. 1). Previously, multiaxial force sensors have required fabrication of individual one dimensional force sensors followed by subsequent three-dimensional assembly processes. However, our approach allows the monolithic manufacturing of multiaxial force sensors without additional assembly or integration steps. Furthermore, depending on the sensor specifications required by the users, we can easily modify the sensor design on-demand and quickly manufacture the sensor product. Thus, our approach will be very useful to quickly fabricate sensors for a number of electronic appliances, toys, household goods, etc. Moreover, TPU and CNT/TPU's flexibility allows a wider deformation range than those of previously reported 3D-printed sensors and therefore would be useful for flexible and wearable electronics applications. For example, it may be suitable for producing low-cost devices that can continuously monitor the degree of patient movement in the rehabilitation process.

## 2. Sensing principle and sensor design

A 3D-printed multiaxial force sensor consists of three orthogonal beams forming a 3D cubic cross shape. This structure is designed to independently detect the multiaxial forces (Fx, Fy, and Fz). Each rectangular beam (beam X, Y, and Z) has the CNT/TPU sensing part (Rx, Ry, and Rz) printed on the surface of TPU beam (Fig. 2a). TPU used in the structural part is nonconductive and flexible with a flexural modulus of 45.2 MPa (refer to Fig. S1 and Table S1 in the Supplementary Information). When the CNT is dispersed into TPU, CNT/TPU composite becomes electrically conductive via percolation network of CNTs in the polymer matrix. When 3D-printed CNT/TPU object is under strain, the number of conduction paths through CNT networks in the composite changes and it results in the piezoresistivity [20–22]. This piezoresistivity of CNT/TPU is the fundamental sensing mechanism of our force sensor.

When Fz+ (downward force in Z axis) is applied to the top of beam X, the force is delivered to the center of 3D cross cubic structure where beams X, Y and Z intersect. Then, beams Y and Z that are simply supported by the supporting frame, undergo bending.

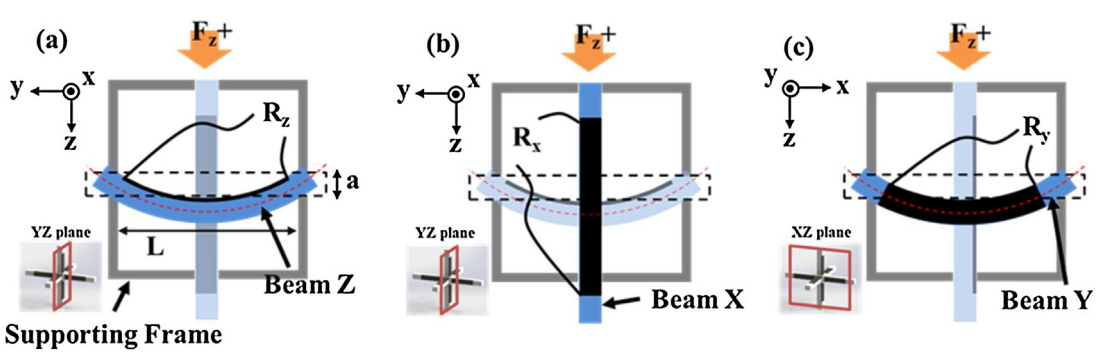


**Fig. 2.** Principle of 3D-printed multiaxial force sensor with an example when Fz+ is applied. (Cross section view, red dash lines indicate the neutral axis of Beam Z. Insets show the cross-section plane under consideration): (a) Rz is under compressive stress by beam bending. (b) Rx is under normal compressive stress by axial loading. (c) Ry is under compressive stress above the neutral axis and under tensile stress below the neutral axis. (For interpretation of the references to colour in this figure legend, the reader is referred to the web version of this article.)

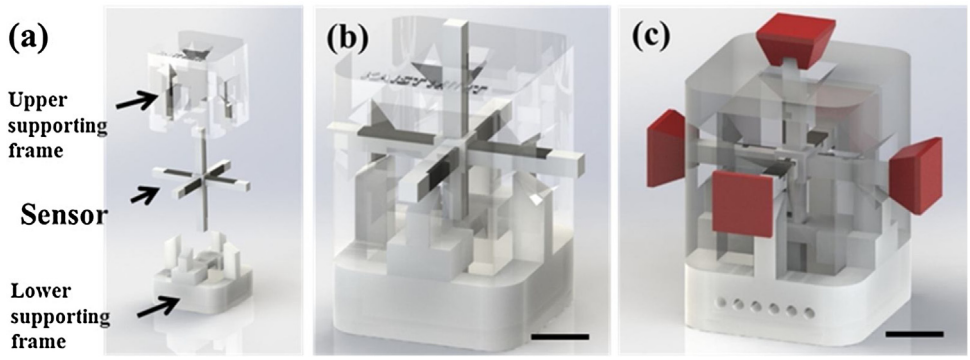


**Fig. 3.** 3D CAD Model of 3D cubic cross multiaxial force sensor: (a) Exploded view of the sensor and the supporting frames. (b) 3D cubic cross multiaxial force sensor assembled with the upper and the lower supporting frames. (c) Assembled sensor with red force pads (Scale bar = 10 mm). (For interpretation of the references to colour in this figure legend, the reader is referred to the web version of this article.)

Finally, Rz on the surface of the beam Z is reduced due to the compressive strain by the downward bending (Fig. 2a). On the other hand, Rx on the surface of beam X changes little as compared to Rz because the normal compressive stress applied on Rx is much less than flexural compressive stress on Rz. When the width and thickness of beam are both 3 mm and length of beam is 20 mm, the ratio of two stresses ($\sigma_n/\sigma_f$) is 0.1 by the following equations:

$$\sigma_n = \frac{F}{a^2}; \textit{normal compressive stress}$$

$$\sigma_f = \frac{3FL}{2a^3}; \textit{flexural compressive stress}$$

Furthermore, since Ry on the surface of beam Y undergoes both compressive and tensile strains (i.e. compressive strain above the neutral axis and tensile strain below the neutral axis) at the same time, the net resistance of Ry exhibits only a negligible change. Therefore, when the Fz+ is given, Rz changes much more significantly than Rx and Ry. In conclusion, the 3D cubic cross shaped force sensor fabricated by 3D printing can detect the forces in three axes with small crosstalk between different axes.

The sensing and structural parts were modeled using 3D CAD program and their dimensions were determined by various factors. First, minimum layer thickness was determined by the sensing principle and the 3D printing quality of the CNT/TPU filament. Since the strain is the largest on the upper or lower surface when the beam is under bending, the sensing part has to be made as thin as possible and printed either on the upper or lower surface to make the resistance change large enough. However, minimum layer thickness offered by the 3D printer is limited to 0.1–0.3 mm. In addition, we found that the 3D printing quality of CNT/TPU filament is not satisfactory if the layer thickness is less than 0.2 mm. Therefore, in order to satisfy the 3D printing quality, the layer thickness was selected to be 0.3 mm. For stable sensor output, the sensing part was printed with two layers (i.e. nominal thickness ~0.6 mm). Second, the 3D-printed multiaxial force sensor was designed to measure forces below 5 N, which corresponds to the range of finger forces [23–25]. We calculated the dimensions of the sensor to withstand the forces required to meet the sensing range while keeping the structural material in the elastic deformation range (Fig. S2). In the view of these requirements, we determined the dimension (width × thickness × length) of the sensing part to be 3 mm × 0.6 mm × 20 mm and that of the structural part to be 3 mm × 2.4 mm × 30 mm.

The 3D-printed multiaxial force sensor can function properly if it is mounted on a supporting frame that provides a simply supported boundary condition for each beam (Fig. 3). Accordingly, we designed the upper and lower supporting frames to hold the sensor in the center when assembled. The supporting edges were designed to be sharp in order to provide simply supported condition in the beam bending. The span between two supports was 20 mm. Six holes were designed in the lower supporting frame for electrical wiring of sensors. The supporting frame was 3D-printed with ABS filament. In addition, the force pads were designed so that the user can easily apply forces along each axis.

## 3. Experiments, results and discussion

### 3.1. CNT/TPU filament fabrication

TPU was chosen as a structural material because it is a thermoplastic polymer that can be used for FDM 3D printing and has much lower stiffness than those of ABS and PLA in order to provide sufficient mechanical flexibility. In our study, we used two types of TPU. One is a commercial TPU filament (Filabot, Korea) for the 3D printing of the structural parts. The other is TPU pellets (Songwon Industry, Korea) for the fabrication of CNT/TPU nanocomposite (The mechanical characteristics of these TPU materials can be found in Table S2). We chose MWCNT (Hyosung, Korea, see Table S3 for material property of utilized CNT) as a conductive filler since it has lower percolation threshold and higher conductivity due to its high aspect ratio [26,27]. Also, they are known to have a good mechanical flexibility [28]. Because CNTs tend to agglomerate together, they have to be well dispersed into the polymer matrix to generate homogenous mechanical and electrical characteristics. We used shear melting process to disperse the CNTs into TPU matrix to overcome the high viscosity of the fluidic TPU [29,30]. A torque rheometer (Haake Rheomix 600) dispersed CNTs by applying thermal energy and shear force to produce the composite material (see Fig. S3 in the Supplementary Information for experimental setup for shear melt process). The thermal energy made TPU to be fluidic and the shear force facilitated dispersion of CNT fillers into the molten TPU. The CNT (1/2/4 wt%) and TPU pellets (Shore hardness 75A, Songwon Industry) were mixed together at 220 °C, 100 rpm for 30 min. Previous studies on the thermogravimetric analysis of nanocomposite/TPU have shown that their weights decreased drastically at the temperatures above 280 °C [31], 250 °C [32] and 300 °C [33]. Therefore, the thermal stability of CNT/TPU nanocomposite could be guaranteed in our mixing process at 220 °C. We were able to measure the electrical resistance of only 4 wt% CNT/TPU using a digital multimeter (Fluke 87 V, USA). This result is consistent with the study of S.D. Ramoa et al. [34]. They found that the CNT/TPU composite with >3 wt% of CNT exhibited much higher conductivity than those of composites with lower CNT contents. After cooling, CNT/TPU composite was pelletized (Fig. 4a). In order to fabricate the composite as a 3D printable filament, pelletized CNT/TPU was

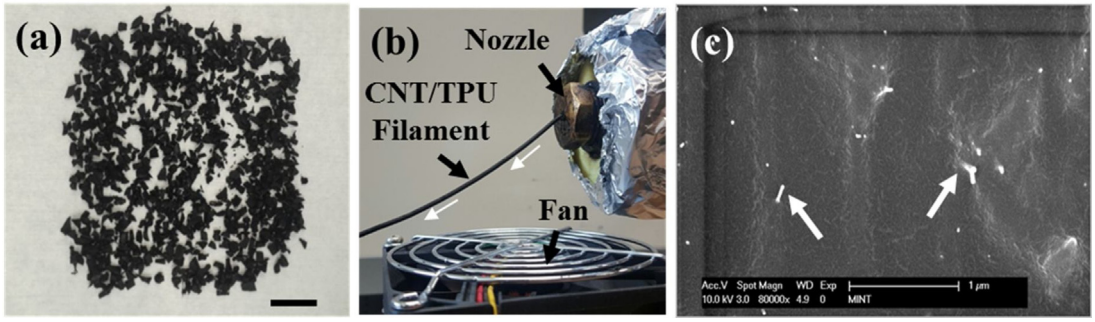


**Fig. 4.** (a) CNT/TPU pellets after shear melt process and pelletizing (Scale bar = 10 mm) (b) Extruded CNT/TPU filament. White arrow indicates the extruding direction. (c) SEM images of CNT/TPU. Arrows indicate the CNTs.

extruded with the filament extruder (Filastruder, USA). The extruding nozzle temperature was set at 190 °C. The average diameter of extruded CNT/TPU filaments was 1.64 mm (standard deviation, SD = 0.049 mm) and the average resistivity of the filament was 0.143 Ω·m (SD = 0.036 Ω m) (Fig. 4b).

### 3.2. Sensor fabrication and characterization

#### 3.2.1. Single beam type sensor

A single beam type sensor was fabricated to characterize the sensing performance of CNT/TPU based piezoresistive sensor. The dimension of the TPU beam was 3 × 2.4 × 30 mm (width × height × length) and that of CNT/TPU was 3 × 0.6 × 30 mm. A single beam sensor was printed with a commercial FDM 3D printer (Makerbot 2X replicator, USA). We used a commercial FDM 3D printer with a dual nozzle system for the sensor fabrication. This dual nozzle system allows the product to be printed with two different materials. The diameter of each nozzle was 0.4 mm. To conduct a three-point bending experiment, two supports and a force applying tip were 3D-printed with ABS. The distance between two supports was 20 mm as shown in Fig. 5a. The tip was attached to the load cell (SM-500N, Interface) and its deflection range and speed were controlled by a linear stage (MA-35, PI, Germany). Two ends of the beam were wired via silver paste for the resistance measurement, which was conducted using an LCR meter (Vac = 1 V, frequency = 1 kHz, Precision LCR meter E4980A, Agilent, USA). When the beam was under bending, the layers of TPU and CNT/TPU showed good interfacial adhesion so that no delamination was observed after the experiments (Fig. S9).

The resistance of the single beam type sensor was measured while the tip pressed down the center by 1 mm at a speed of 0.1 mm/s. Simultaneously, the force needed to bend the beam was recorded using a load cell. The initial resistance of 10.92 kΩ was decreased to 9.76 kΩ (10.6% decrease) after 1 mm deflection by a load of Fz = 2.11 N (Fig. 5b). At the early stage of loading, the slope of force was relatively lower than the average slope, which is assumed to be due to the loose initial contact between the tip and beam. Due to the viscoelastic behavior of TPU, the beam did not fully recover to the initial state when the tip returned to the original position (Refer to Fig. S4 in the Supplementary Information for force-deflection curve of single beam sensor). In case of the resistance, the slope of the resistance change was small at the beginning and end of the deflection. This may be because conformal contact gradually occurred in the early stage and the nonlinear behavior of piezoresistivity appeared at the center in the last stage. Also, as shown in Fig. 5c, viscoelastic property of the structural and sensing materials caused hysteresis of resistance vs. force curve. In the cyclic bending test with the deflection of 0.5 mm and a speed of 1 mm/s, the sensor showed drifting behavior that can also be attributed to the viscoelastic property of structural and sensing materials (Fig. 5d). During the 1–1000 cycles, the base resistance decreased by 0.65%. The rate of drifting slowly decreased as the number of cycle increased, which is commonly observed in CNT/polymer composite because new conductive pathways are accumulated as the unrecovered plastic deformation exists [35,36]. In addition, the responses of single beam sensor to different deflection speeds were characterized as shown in Fig. 5e. It is observed that the resistance change becomes slightly smaller at higher deflection speed (i.e. higher strain rate). When the velocity was 0.1 mm/s, the maximum resistance change was 0.55%. However, when the velocity was 2 mm/s, it was 0.52%. This could be also due to the viscoelastic behaviors of TPU and CNT/TPU composite that may delay the re-arrangement of CNT networks.

#### 3.2.2. 3D cubic cross multiaxial force sensor

With the basic knowledge about the printing conditions and preliminary results of single beam type force sensor, we designed and fabricated 3D cubic cross multiaxial force sensor. First, we drew the sensing and structural parts using 3D CAD program as shown in Fig. 3. 3D cubic cross structure was drawn considering the empty spaces where the sensing part will be printed. A small TPU cube was designed to stabilize the structure at the center where three beams intersect. 3D cubic cross shaped structure and the sensing part were printed with TPU and CNT/TPU, respectively. Then, 3D printing conditions were set for each filament for optimal 3D printing quality. TPU and CNT/TPU filaments were printed at 200 °C and 230 °C, respectively. The printing speed was 30 mm/s and the heating bed temperature was set at 70 °C (Fig. S5). Because the beam X and Z are located above the printing floor, supporting structure was printed under those beams with TPU. It took 30 min to complete the 3D printing process of the entire cross cubic structure with multiaxial force sensors (Fig. 6a). After the 3D printing, the supporting structure and debris made during the process were removed. Afterwards, electrical wires were connected on each end of the sensing parts using a silver paste, followed by curing at 120 °C for 20 min.

Stacked layers of 3D-printed TPU and CNT/TPU can be observed in Fig. 6b. The initial values of Rz, Ry, and Rx were 291.5 kΩ, 87.2 kΩ, and 323 kΩ, respectively. Two features of FDM 3D printing affected the initial resistance of the fabricated sensor. One is that each layer is stacked in the Z direction, and the other is that the filaments are extracted along a specific printing path through the nozzle. Since the structure is completed by stacking layers in the Z-axis direction, Rz and Ry are completed with only two and ten layers, respectively. On the other hand, since Rx is directed along the Z axis, one hundred layers must be stacked on the Z axis to complete the structure. As a result, the CNT/TPU filaments were printed alternately several times with the TPU filaments and some printed surface appeared to be quite rough for Rx (See Fig. S6(a)). Because of this reason, the resistance of Rx was finally larger than Ry and Rz. However, when other 3D printing technologies such as multi-material poly-

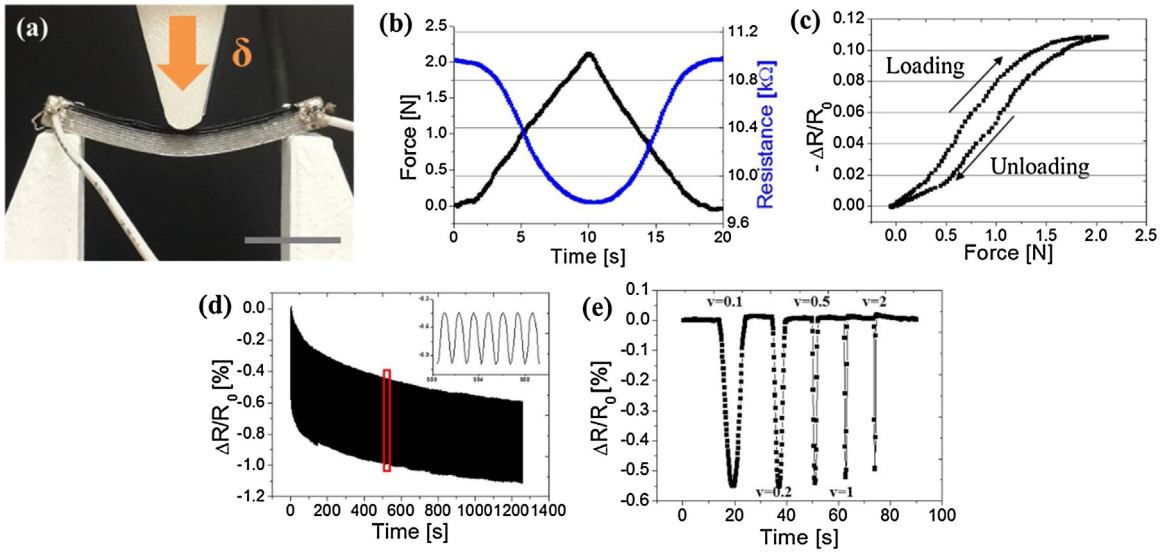


**Fig. 5.** Single beam type sensor for the characterization of the sensing performance of CNT/TPU based piezoresistive sensor: (a) Three-point bending test with resistance measurement (Scale bar = 10 mm); (b) Force and resistance measurement during 1 mm deflection and recovery at a speed of 0.1 mm/s; (c) Curve of force vs. resistance change; (d) Response to repeated bending cycles (1000 times, maximum deflection of 0.5 mm and speed of 1 mm/s); (e) Response to different deflection speeds (maximum deflection of 0.5 mm, and speed of 0.1, 0.2, 0.5, 1.0, and 2.0 mm/s).

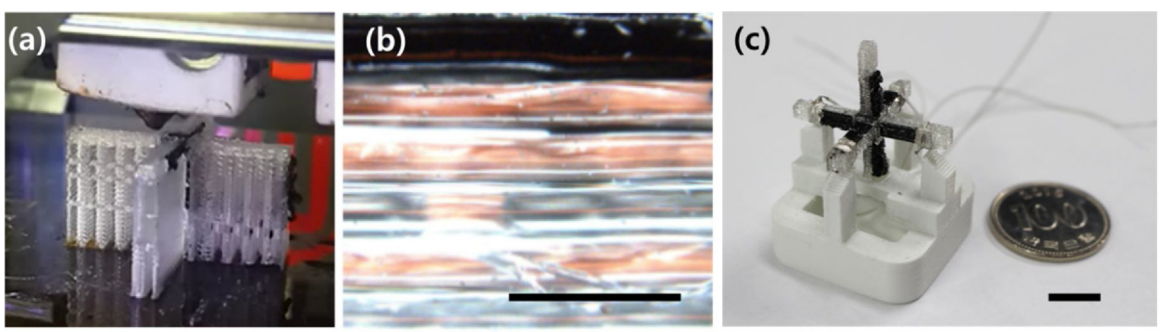


**Fig. 6.** Fabrication of 3D cubic cross force sensor: (a) 3D printing of the sensor with commercial FDM 3D printer, (b) Cross-sectional microscopic image of Beam Z (Scale bar = 1 mm), (c) Sensor mounted on the lower supporting frame (Scale bar = 10 mm).

jet printing that could overcome the limitation of FDM 3D printing resolution of functional materials are utilized, the fabricated sensor would have much more stable sensing performance and uniform structures. The difference between Ry and Rz is mainly due to the difference in the printing path. Rz is fabricated by printing the borders first and then filling inside along diagonal direction (See Fig. S6(b)). On the other hand, for the fabrication of Ry, single layer is completed with two connected lines and these layers were piled up in the Z axis (See Fig. S6(c)). Therefore, when the resistances are measured in the longitudinal direction, the conducting path Ry is much well-aligned than Rz, resulting in smaller value of Ry than Rz.

To investigate the characteristics of 3D-printed multiaxial force sensor, we performed a bending test. We fabricated four testing supports that can provide simply supported boundary conditions. The top of beam X was then pressed down by 1 mm at a rate of 0.1 mm/s through a flat acryl plate by applying Fz+. (Fig. 7a) When we applied a load to the sensor, the deflection and force showed a linear relationship. The maximum Fz to cause the deflection of 1 mm was measured as 4 N (Fig. 7b), while Fx and Fy were 3.46 N and 3.66 N, respectively, for the same amount of deflection. This inequality is due to the anisotropic flexural modulus of the consisting beams, coupled 3D structure of the sensor, and 3D-printing direction of CNT/TPU and TPU layers. On the other hand, small hysteresis was observed during the loading and unloading cycles due to the viscoelastic behavior of TPU (Fig. 7c), which was also observed in the single beam sensor experiment (Fig. S4).

As shown in Fig. 7d, when Fz+ is applied and a deflection of 1 mm is generated, Rz and Ry decreased by 2% and 0.2%, respectively, which verifies that our sensor could independently measure the multiaxial force with small crosstalk. However, the resistance changes of multiaxial force sensor did not appear much compared to the results of single beam sensor. In specific, only a change of 2% was observed in multiaxial force sensor as compared with the single beam sensor with a change of 10.6% by a deflection of 1 mm. This is due to the different geometry of the 3D cubic cross sensor. In the case of a single beam type sensor, when a force is applied to the center, most area of the sensing part bend uniformly at the same time. However, the 3D cubic cross sensor has a structure in which three beams are connected at the center. In addition, there is an additional TPU cubic structure at the intersection of three beams. This prevent the bending of the sensing part at the center where the maximum stress has to occur. As a result, the resistance change in the 3D cubic cross sensor was less than that in the single beam type sensor. Also, we found that there is a drift of resistance in the cyclic test. In the first ten cycles, the baseline value of Rz under Fz = 0 was reduced by 1%, which may have happened due to the viscoelastic behavior of TPU and CNT/TPU. Although the CNT networks in TPU matrix require a certain time to recover, loading and unloading cycle occurred in a short period.

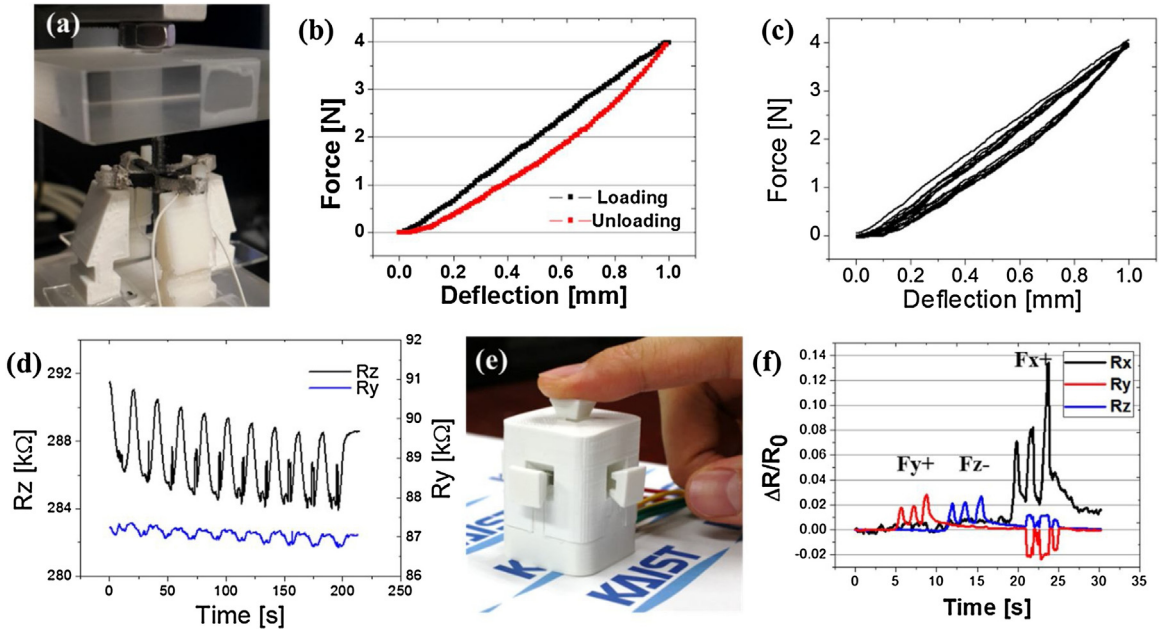


**Fig. 7.** Characterization of 3D cubic cross force sensor: (a) Experimental setup for the characterization of force-deflection curve of 3D-printed multiaxial force sensor, (b-c) Force vs. deflection for single and multiple cycles of loading-unloading, (d) Rz and Ry under 1 mm cyclic deflection in Z axis, (e) 3D-printed multiaxial force sensor assembly as a three axis haptic device, (f) Real-time resistance change of Rx, Ry, and Rz when Fy+, Fz- and Fx+ were applied in series.

After the sensor characterization, we developed a haptic device based on a 3D-printed multiaxial force sensor (Fig. 7e). We designed multichannel sensing system with data acquisition (DAQ) device (NI cDAQ-9178, National Instruments) and voltage dividing circuit. When the sensor and reference resistors are connected in series and DC voltage is applied, sensor resistance change can be calculated by measuring the voltage across the reference resistance. Since the three sensing parts meet in the middle, a circuit that can measure individual resistances by switching the resistors in each direction was constructed. Fig. 7f shows the resistance change of Rx, Ry and Rz monitored in real time through this measurement system. We sequentially applied Fy+, Fz-, and Fx+ by three times each. When Fy+ was given, only Ry changed by 2.0–2.8%. When Fz- was given, only Rz increased by 2.4–2.7%. When Fx+ was given, Rx increased by 8.1–11.2%. After each initial loading, the base resistances were increased due to the viscoelastic behavior of the material. Also, the change of Rx was larger than the other two resistors. It seems that because the 3D printing quality in Z direction was comparably poor than the others, the shape of the Rx was not uniform. Concentrated stresses on the border of each layer appear to have caused larger resistance change in Rx under Fx than Ry under Fy or Rz under Fz. The crosstalk was not negligibly small as designed. Rx changed about 0.4% by Fz, and Ry and Rz changed by 1% and 2%, respectively by Fx. It was due to the connection of the sensing parts at the center and some non-uniform structure of the 3D-printed parts. However, we could find that the changing ratio of the resistance was smaller when it was deformed by other force components (Fy and Fz).

## 4. Conclusion

In this paper, we developed a novel method for the direct fabrication of multiaxial force sensors by 3D printing of functional materials. By simultaneous 3D printing of structural and sensing materials, we could easily fabricate 3D structures with sensing functions. We have demonstrated the potential usage of flexible polymer as a structural material for multiaxial force sensors, while its viscoelastic property sacrifices dynamic characteristics and stability of the sensor with a certain level of hysteresis. We also have verified that the nanocomposite of CNT and thermoplastic polymer can be utilized for the direct 3D printing of piezoresistive sensors in 3D space. Previously, multiaxial force sensors could be fabricated by a sequential process: fabrication of individual sensors followed by their 3D assembly. However, our method has enabled the monolithic manufacturing process of multiaxial 3D force sensors without additional assembly or integration processes by taking advantage of multi-nozzle 3D printing. Furthermore, depending on the sensor specifications required by the users, we can easily modify the design and material for the sensors. Therefore, our approach will be very useful to quickly fabricate sensors for a number of electrical and mechanical applications. Moreover, if a variety of functional composites are developed, force sensors can be implemented with a variety of other sensing principles. In addition, when the limitations of FDM 3D printing such as low printing resolution and poor printability of composite materials are resolved with other 3D printing methods, more functional products with integrated sensing capabilities can be manufactured using our approach.

## Acknowledgements

Prof. Jae Wook Lee and Mr. Jong Han Choi in Applied Rheology Laboratory at Sogang University helped to produce CNT/TPU composites. This work was supported by the Industrial Strategic Technology Development Program (10041618, Development of Needle Insertion Type Image-based Interventional Robotic System for Biopsy and Treatment of 1 cm abdominal and Thoracic Lesion with Reduced Radiation Exposure and Improved Accuracy) funded by the Ministry of Trade Industry and Energy (MOTIE, Korea) and by Nano-Convergence Foundation (www.nanotech2020.org) funded by the Ministry of Science, ICT and Future Planning (MSIP, Korea) & MOTIE [Project number: R201603110].

## Appendix A. Supplementary data

Supplementary data associated with this article can be found, in the online version, at http://dx.doi.org/10.1016/j.sna.2017.07.020.

## References


[1] U. Kalsoom, P.N. Nesterenko, B. Paull, Recent developments in 3D printable composite materials, RSC Adv. 6 (2016) 60355–60371.
[2] R.D. Farahani, M. Dubé, D. Therriault, Three-dimensional printing of multifunctional nanocomposites: manufacturing techniques and applications, Adv. Mater. 28 (2016) 5794–5821.
[3] C. Shemelya, F. Cedillos, E. Aguilera, E. Maestas, J. Ramos, D. Espalin, et al., 3D printed capacitive sensors, Sensors IEEE (2013) 1–4.
[4] D. Espalin, D.W. Muse, E. MacDonald, R.B. Wicker, 3D printing multifunctionality: structures with electronics, Int. J. Adv. Manuf. Technol. 72 (2014) 963–978.
[5] C. Shemelya, L. Banuelos-Chacon, A. Melendez, C. Kief, D. Espalin, R. Wicker, et al., Multi-functional 3D printed and embedded sensors for satellite qualification structures, Sensors IEEE (2015) 1–4.
[6] H. Ota, S. Emaminejad, Y. Gao, A. Zhao, E. Wu, S. Challa, et al., Application of 3D printing for smart objects with embedded electronic sensors and systems, Adv. Mater. Technol. 1 (2016), 1600013.
[7] S.-Y. Wu, C. Yang, W. Hsu, L. Lin, 3D-printed microelectronics for integrated circuitry and passive wireless sensors, Microsyst. Nanoeng. 1 (2015).
[8] H. Peng, F. Guimbretière, J. McCann, S. Hudson, A 3D printer for interactive electromagnetic devices, Proceedings of the 29th Annual Symposium on User Interface Software and Technology, ACM (2016) 553–562.
[9] K. Nate, M.M. Tentzeris, A novel 3-D printed loop antenna using flexible NinjaFlex material for wearable and IoT applications, Electrical Performance of Electronic Packaging and Systems (EPEPS), 2015 IEEE 24th, IEEE (2015) 171–174.
[10] P.K. Yuen, Embedding objects during 3D printing to add new functionalities, Biomicrofluidics 10 (2016) 044104.
[11] A. Le Duigou, M. Castro, R. Bevan, N. Martin, 3D printing of wood fibre biocomposites: from mechanical to actuation functionality, Mater. Design 96 (2016) 106–114.
[12] D.C. Zuluaga, A. Menges, 3D printed hygroscopic programmable material systems, in: MRS Proceedings, Cambridge Univ Press, 2015, pp. mrss15-2134303.
[13] M. Schmitz, M. Khalilbeigi, M. Balwierz, R. Lissermann, M. Mühlhäuser, J. Steimle, Capricate: a fabrication pipeline to design and 3D print capacitive touch sensors for interactive objects, Proceedings of the 28th Annual ACM Symposium on User Interface Software & Technology, ACM (2015) 253–258.
[14] G. Postiglione, G. Natale, G. Griffini, M. Levi, S. Turri, Conductive 3D microstructures by direct 3D printing of polymer/carbon nanotube nanocomposites via liquid deposition modeling, Compos. Part A: Appl. Sci. Manuf. 76 (2015) 110–114.
[15] S. Leigh, Polymer composites for 3D printing of functional sensors and transducers, Sensors IEEE (2016) 1–3.
[16] Z. Rymansaib, P. Iravani, E. Emslie, M. Medvidović-Kosanović, M. Sak-Bosnar, R. Verdejo, et al., All-polystyrene 3D-printed electrochemical device with embedded carbon nanofiber-graphite-polystyrene composite conductor, Electroanalysis 28 (7) (2016) 1517–1523.
[17] K. Chizari, M.A. Daoud, A.R. Ravindran, D. Therriault, 3D printing of highly conductive nanocomposites for the functional optimization of liquid sensors, Small 12 (2016) 6076–6082.
[18] S.-z. Guo, X. Yang, M.-C. Heuzey, D. Therriault, 3D printing of a multifunctional nanocomposite helical liquid sensor, Nanoscale 7 (2015) 6451–6456.
[19] G.I. Peterson, M.B. Larsen, M.A. Ganter, D.W. Storti, A.J. Boydston, 3D-printed mechanochromic materials, ACS Appl. Mater. Interfaces 7 (2014) 577–583.
[20] M. Melnykowycz, B. Koll, D. Scharf, F. Clemens, Comparison of piezoresistive monofilament polymer sensors, Sensors 14 (2014) 1278–1294.
[21] K. Shehzad, J.-W. Zha, Z.-F. Zhang, J.-K. Yuan, Z.-M. Dang, Piezoresistive behavior of electrically conductive carbon fillers/thermoplastic elastomer nanocomposites, J. Adv. Phys. 2 (2013) 70–74.
[22] W. Obitayo, T. Liu, A review: carbon nanotube-based piezoresistive strain sensors, J. Sens. 2012 (2012).
[23] M. Fontana, S. Marcheschi, F. Salsedo, M. Bergamasco, A three-axis force sensor for dual finger haptic interfaces, Sensors 12 (2012) 13598–13616.
[24] R.D.P. Wong, J.D. Posner, V.J. Santos, Flexible microfluidic normal force sensor skin for tactile feedback, Sens. Actuators A: Phys. 179 (2012) 62–69.
[25] M. Vatani, Y. Lu, E.D. Engeberg, J.-W. Choi, Combined 3D printing technologies and material for fabrication of tactile sensors, Int. J. Precis. Eng. Manuf. 16 (2015) 1375–1383.
[26] P. Pötschke, L. Häußler, S. Pegel, R. Steinberger, G. Scholz, Thermoplastic polyurethane filled with carbon nanotubes for electrical dissipative and conductive applications, KGK Kautschuk Gummi Kunststoffe 60 (2007) 432–437.
[27] K. Shehzad, Z.-M. Dang, M.N. Ahmad, R.U.R. Sagar, S. Butt, M.U. Farooq, et al., Effects of carbon nanotubes aspect ratio on the qualitative and quantitative aspects of frequency response of electrical conductivity and dielectric permittivity in the carbon nanotube/polymer composites, Carbon 54 (2013) 105–112.
[28] J.-P. Salvetat, J.-M. Bonard, N. Thomson, A. Kulik, L. Forro, W. Benoit, et al., Mechanical properties of carbon nanotubes, Appl. Phys. A 69 (1999) 255–260.
[29] S. Cravanzola, G. Haznedar, D. Scarano, A. Zecchina, F. Cesano, Carbon-based piezoresistive polymer composites: structure and electrical properties, Carbon 62 (2013) 270–277.
[30] Z.-M. Dang, K. Shehzad, J.-W. Zha, A. Mujahid, T. Hussain, J. Nie, et al., Complementary percolation characteristics of carbon fillers based electrically percolative thermoplastic elastomer composites, Compos. Sci. Technol. 72 (2011) 28–35.
[31] M. Fonseca, B. Abreu, F. Gonçalves, A. Ferreira, R. Moreira, M. Oliveira, Shape memory polyurethanes reinforced with carbon nanotubes, Compos. Struct. 99 (2013) 105–111.
[32] A.K. Barick, D.K. Tripathy, Effect of nanofiber on material properties of vapor-grown carbon nanofiber reinforced thermoplastic polyurethane (TPU/CNF) nanocomposites prepared by melt compounding, Compos. Part A: Appl. Sci. Manuf. 41 (2010) 1471–1482.
[33] H. Quan, B.-q. Zhang, Q. Zhao, R.K. Yuen, R.K. Li, Facile preparation and thermal degradation studies of graphite nanoplatelets (GNPs) filled thermoplastic polyurethane (TPU) nanocomposites, Compos. Part A: Appl. Sci. Manuf. 40 (2009) 1506–1513.
[34] S.D. Ramôa, G.M. Barra, R.V. Oliveira, M.G. de Oliveira, M. Cossa, B.G. Soares, Electrical, rheological and electromagnetic interference shielding properties of thermoplastic polyurethane/carbon nanotube composites, Polym. Int. 62 (2013) 1477–1484.
[35] H. Liu, 刘虎, W. Huang, 黄文举, J. Gao, 高嘉辰, et al., Piezoresistive behavior of porous carbon nanotube-thermoplastic polyurethane conductive nanocomposites with ultrahigh compressibility, Applied Physics Letters, 108 (2016) 011904.
[36] R. Zhang, H. Deng, R. Valenca, J. Jin, Q. Fu, E. Bilotti, et al., Strain sensing behaviour of elastomeric composite films containing carbon nanotubes under cyclic loading, Compos. Sci. Technol. 74 (2013) 1–5.


## Biographies

**Kyuyoung Kim** received B.S. in mechanical engineering from KAIST, Korea (2014), and M.S. in mechanical engineering from KAIST, Korea (2016). He is currently a doctoral student at KAIST. His main research interests are micro/nano fabrication based multifunctional sensors and 3D-printed sensors with functionalized composite materials.

**Jaeho Park** received B.S. in mechanical engineering from Hanyang University, Korea (2013), and M.S. in mechanical engineering from KAIST, Korea. He is currently a doctoral student at KAIST. His main research interest is a flexible micro physical/chemical sensor towards sensor integrated smart medical systems.

**Ji-hoon Suh** received B.S. degree from Chung-Ang University, Korea(2013) and M.S. degree from KAIST, Korea (2016), both in Electrical Engineering. His current research interests are on multiparameter sensor interface circuits and embedded systems for sensor applications. He is currently a researcher at KAIST.

**Minseong Kim** received the B.S. in nanomechatronics engineering from Pusan National University, Korea (2014), and M.S. in mechanical engineering from KAIST, Korea (2016). He is currently a doctoral student at KAIST. His research interests are flexible sensor, stretchable sensor, electronic skin and wearable devices.

**Yongrok Jeong** received the B.S. in mechanical engineering from KAIST, Korea (2016). He is currently a master student at KAIST. His main research interests are smart material based transducer and micro/nano fabricated transducer.

**Dr. Inkyu Park** received his B.S., M.S., and Ph.D. from KAIST (1998), UIUC (2003) and UC Berkeley (2007), respectively, all in mechanical engineering. He has been with the department of mechanical engineering at KAIST since 2009 as a faculty and is currently an associate professor. His research interests are nanofabrication, smart sensors, nanomaterial-based sensors and flexible & wearable electronics. He has published more than 60 international journal articles (SCI indexed) and 100 international conference proceeding papers in the area of MEMS/NANO engineering. He is a recipient of IEEE NANO Best Paper Award (2010) and HP Open Innovation Research Award (2009–2012).